Article

Phosphorescent Platinum Acetylide Organogelators

Thomas Cardolaccia, Yongjun Li, and Kirk S. Schanze

J. Am. Chem. Soc., **2008**, 130 (8), 2535-2545 • DOI: 10.1021/ja0765316

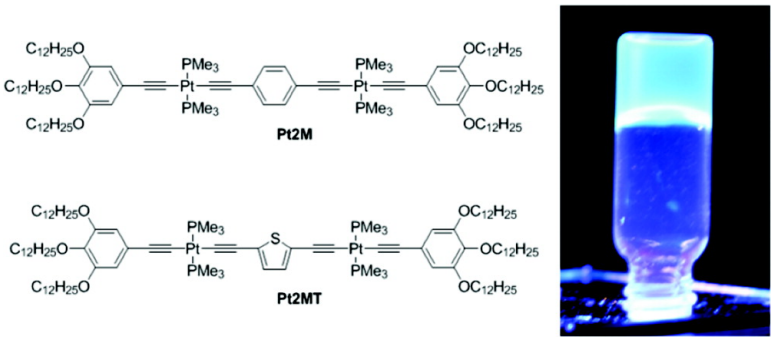

More About This Article

Additional resources and features associated with this article are available within the HTML version:

- Supporting Information
- Links to the 8 articles that cite this article, as of the time of this article download
- Access to high resolution figures
- Links to articles and content related to this article
- Copyright permission to reproduce figures and/or text from this article

View the Full Text HTML

J|A|C|S
ARTICLES
Published on Web 01/31/2008

Phosphorescent Platinum Acetylide Organogelators

Thomas Cardolaccia, Yongjun Li, and Kirk S. Schanze*

Department of Chemistry, University of Florida, P.O. Box 117200, Gainesville, Florida 32611

Received August 29, 2007; Revised Manuscript Received December 13, 2007; E-mail: kschanze@chem.ufl.edu

Abstract: The series of platinum acetylide oligomers (PAOs) with the general structure *trans,trans*-[$(RO)_3Ph{-}C{\equiv}C{-}Pt(PMe_3)_2{-}C{\equiv}C{-}(Ar){-}C{\equiv}C{-}Pt(PMe_3)_2{-}C{\equiv}C{-}Ph(OR)_3$], where Ar = 1,4-phenylene, 2,5-thienylene, or bis-2,5-(*S*-2-methylbutoxy)-1,4-phenylene and R = *n*-$C_{12}H_{25}$ gel hydrocarbon solvents at concentrations above 1 mM. Gelation is thermally reversible ($T_{gel-sol} \approx 40-50$ °C), and it occurs due to aggregation of the PAOs resulting in the formation of a fibrous network that is observed for dried gels imaged by TEM. The influence of aggregation/gelation on the photophysical properties of the PAOs is explored in detail. Aggregation induces a significant blue shift in the oligomers' absorption spectra, and the shift is attributed to exciton interactions arising from H-aggregation of the chromophores. Strong circular dichroism (CD) is observed for gelled solutions of a PAO substituted with homochiral *S*-2-methylbutoxy side chains on the central phenylene unit. The CD is attributed to formation of a chiral supramolecular aggregate structure. The PAOs are phosphorescent at ambient temperature in solution and in the aggregate/gel state. The phosphorescence band is blue-shifted ca. 20 nm in the aggregate/gel, and the shift is assigned to emission from an unrelaxed conformation of the triplet excited state. Phosphorescence spectroscopy of mixed aggregate/gels consisting of a triplet donor/host oligomer (Ar = 1,4-phenylene) doped with low concentrations of an acceptor/trap oligomer (Ar = 2,5-thienylene) indicates that energy transfer occurs efficiently in the aggregates. Triplet energy transfer involves exciton diffusion among the host chromophores followed by Dexter exchange energy transfer to the trap chromophore.

Introduction

The performance of organic electronic devices such as light emitting diodes, photovoltaic cells, and field effect transistors that rely on π-conjugated oligomers or polymers as active materials depends on the intrinsic optical and electronic properties of the constituent molecules as well as intermolecular interactions and morphology of the solid-state material. While molecular optical and electronic properties have received the most attention, supramolecular interactions and material morphology are arguably more important in determining the performance of an organic material in device applications.[1,2] Controlling self-assembly of π-conjugated molecular systems is important as it provides an avenue to organic materials having desired optical, electronic, and optoelectronic properties.[3] Recent investigations of self-assembly of π-conjugated polymers and oligomers into supramolecular aggregates and gels have provided considerable insight into the structural factors that are important in producing assemblies with long range order.[4−42] Self-assembly of π-conjugated systems occurs mainly due to van der Waals, hydrogen-bond, and solvophobic interactions among the constituent units.[3]

Suitably functionalized derivatives of oligo(phenylene vinylene)[4,6−8,10,11] and oligo(phenylene ethynylene)[14,15] self-assemble in solution, producing helical or lamellar supramolecular structures that sometimes induce gelation. Many of these supramolecular structures are chiral, as evidenced by the observation of strong ellipticity in circular dichroism spectra.[3,6,20] The supramolecular aggregates and gels consisting of π-conjugated oligomers provide ideal platforms for the study of phenomena that are usually only encountered in solid-state materials. For example charge carrier mobility,[25,43,44] exciton

(1) Müllen, K.; Wegner, G. *Electronic Materials: The Oligomer Approach*; Wiley-VCH: Weinheim, 1998.
(2) Martin, R. E.; Diederich, F. *Angew. Chem., Int. Ed.* **1999**, *38*, 1350−1377.
(3) Hoeben, F. J. M.; Jonkheijm, P.; Meijer, E. W.; Schenning, A. P. H. J. *Chem. Rev.* **2005**, *105*, 1491−1546.
(4) Schenning, A. P. H. J.; Jonkheijm, P.; Peeters, E.; Meijer, E. W. *J. Am. Chem. Soc.* **2001**, *123*, 409−416.
(5) Würthner, F.; Chen, Z.; Hoeben, F. J. M.; Osswald, P.; You, C.-C.; Jonkheijm, P.; Herrikhuyzen, J. v.; Schenning, A. P. H. J.; van der Schoot, P. P. A. M.; Meijer, E. W.; Beckers, E. H. A.; Meskers, S. C. J.; Janssen, R. A. J. *J. Am. Chem. Soc.* **2004**, *126*, 10611−10618.
(6) Jonkheijm, P.; van der Schoot, P.; Schenning, A.; Meijer, E. W. *Science* **2006**, *313*, 80−83.
(7) Zhang, H.; Hoeben, F. J. M.; Pouderoijen, M. J.; Schenning, A.; Meijer, E. W.; Schryver, F. C.; De Feyter, S. *Chem.—Eur. J.* **2006**, *12*, 9046−9055.
(8) Hulvat, J. F.; Sofos, M.; Tajima, K.; Stupp, S. I. *J. Am. Chem. Soc.* **2005**, *127*, 366−372.
(9) Tajima, K.; Li, L. S.; Stupp, S. I. *J. Am. Chem. Soc.* **2006**, *128*, 5488−5495.
(10) Ajayaghosh, A.; George, S. J. *J. Am. Chem. Soc.* **2001**, *123*, 5148−5149.
(11) Ajayaghosh, A.; George, S. J.; Praveen, V. K. *Angew. Chem., Int. Ed.* **2003**, *42*, 332−335.
(12) George, S. J.; Ajayaghosh, A.; Jonkheijm, P.; Schenning, A.; Meijer, E. W. *Angew. Chem., Int. Ed.* **2004**, *43*, 3422−3425.
(13) Ajayaghosh, A.; Varghese, R.; George, S. J.; Vijayakumar, C. *Angew. Chem., Int. Ed.* **2006**, *45*, 1141−1144.
(14) Ajayaghosh, A.; Varghese, R.; Mahesh, S.; Praveen, V. K. *Angew. Chem., Int. Ed.* **2006**, *45*, 7729−7732.
(15) Ajayaghosh, A.; Varghese, R.; Praveen, V. K.; Mahesh, S. *Angew. Chem., Int. Ed.* **2006**, *45*, 3261−3264.
(16) Ajayaghosh, A.; Vijayakumar, C.; Praveen, V. K.; Babu, S. S.; Varghese, R. *J. Am. Chem. Soc.* **2006**, *128*, 7174−7175.
(17) Praveen, V. K.; George, S. J.; Ajayaghosh, A. *Macromol. Symp.* **2006**, *241*, 1−8.
(18) van de Craats, A. M.; Warman, J. M.; Fechtenkotter, A.; Brand, J. D.; Harbison, M. A.; Mullen, K. *Adv. Mater.* **1999**, *11*, 1469−1472.

diffusion,[45−47] and excited-state energy transfer within aggregates consisting of π-conjugated molecular units[11,18,48] have been studied by using solution-based techniques.

While considerable work has been carried out on supramolecular structures comprised of organic π-conjugated systems, relatively few studies have explored the properties of aggregates or gels consisting of metal-organic or organometallic π-conjugated oligomers or polymers.[49−53] These systems are of interest, as introduction of metal centers into optical or electronic materials can have a profound influence on their performance.[54−56] Inspired in part by the reports of the self-assembly properties of suitably substituted π-conjugated oligomers reported by Meijer, Stupp, Ajaygosh, and others,[3,4,8,10,15,20] we designed the series of platinum acetylide oligomers (PAOs) shown in Chart 1 with the objective of studying the properties of the constituent oligomers in supramolecular aggregate structures. The PAO structures consist of a π-conjugated, rigid rod core moiety capped on either end with tri(dodecyloxy)phenyl units. On the basis of earlier work with structurally similar organic analogues, the PAOs were anticipated to aggregate in, and possibly gel, hydrocarbon solvents. The PAOs feature a π-conjugated platinum acetylide chromophore that absorbs light strongly in the near-UV and exhibits room-temperature phosphorescence from a long-lived triplet excited state that is produced with near unit quantum efficiency following photoexcitation.[57−62] Importantly, the existence of phosphorescence allows investigation of the behavior of the triplet exciton in supramolecular aggregates, e.g., triplet excimer formation and triplet exciton diffusion and triplet−triplet energy transfer.

Although there have been investigations of triplet energy transfer in molecular crystals,[63,64] few studies of triplet energy

Chart 1

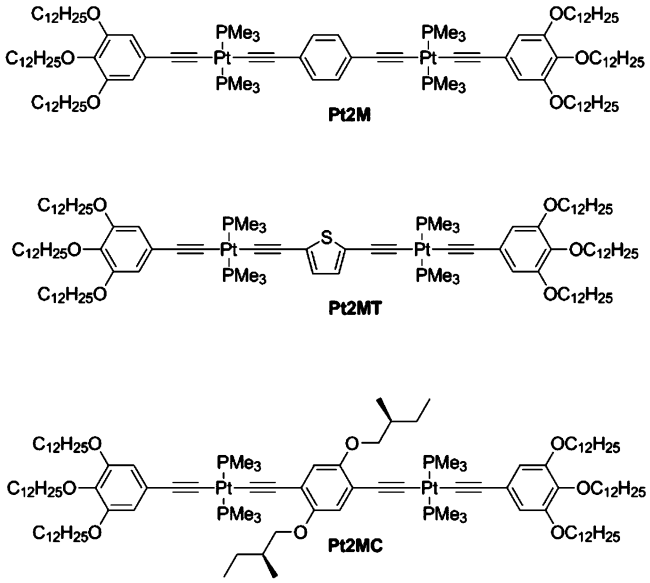

(19) Prins, P.; Senthilkumar, K.; Grozema, F. C.; Jonkheijm, P.; Schenning, A.; Meijer, E. W.; Siebbeles, L. D. A. *J. Phys. Chem. B* **2005**, *109*, 18267−18274.
(20) Herz, L. M.; Daniel, C.; Silva, C.; Hoeben, F. J. M.; Schenning, A. P. H. J.; Meijer, E. W.; Friend, R. H.; Phillips, R. T. *Phys. Rev. B: Condens. Matter* **2003**, *68*, 045203.
(21) Beljonne, D.; Hennebicq, E.; Daniel, C.; Herz, L. M.; Silva, C.; Scholes, G. D.; Hoeben, F. J. M.; Jonkheijm, P.; Schenning, A. P. H. J.; Meskers, S. C. J.; Philips, R. T.; Friend, R. H.; Meijer, E. W. *J. Phys. Chem. B* **2005**, *109*, 10594−10604.
(22) Daniel, C.; Herz, L. M.; Silva, C. *Phys. Rev. B: Condens. Matter* **2003**, *68*, 235212.
(23) Hoeben, F. J. M.; Herz, L. M.; Daniel, C.; Jonkheijm, P.; Schenning, A. P. H. J.; Silva, C.; Meskers, S. C. J.; Beljonne, D.; Phillips, R. T.; Friend, R. H.; Meijer, E. W. *Angew. Chem., Int. Ed.* **2004**, *43*, 1976−1979.
(24) Praveen, V. K.; George, S. J.; Varghese, R.; Vijayakumar, C.; Ajayaghosh, A. *J. Am. Chem. Soc.* **2006**, *128*, 7542−7550.
(25) Ajayaghosh, A.; Praveen, V. K.; Srinivasan, S.; Varghese, R. *Adv. Mater.* **2007**, *19*, 411−415.
(26) Ajayaghosh, A.; Praveen, V. K. *Acc. Chem. Res.* **2007**, *40*, 644−656.
(27) Huber, V.; Katterle, M.; Lysetska, M.; Würthner, F. *Angew. Chem., Int. Ed.* **2005**, *44*, 3147−3151.
(28) Wurthner, F.; Chen, Z. J.; Dehm, V.; Stepanenko, V. *Chem. Commun.* **2006**, 1188−1190.
(29) Zhang, X.; Chen, Z. J.; Wurthner, F. *J. Am. Chem. Soc.* **2007**, *129*, 4886−4887.
(30) Dehm, V.; Chen, Z. J.; Baumeister, U.; Prins, P.; Siebbeles, L. D. A.; Wurthner, F. *Org. Lett.* **2007**, *9*, 1085−1088.
(31) Chen, Z. J.; Stepanenko, V.; Dehm, V.; Prins, P.; Siebbeles, L. D. A.; Seibt, J.; Marquetand, P.; Engel, V.; Wurthner, F. *Chem.—Eur. J.* **2007**, *13*, 436−449.
(32) Sinks, L. E.; Rybtchinski, B.; Iimura, M.; Jones, B. A.; Goshe, A. J.; Zuo, X. B.; Tiede, D. M.; Li, X. Y.; Wasielewski, M. R. *Chem. Mater.* **2005**, *17*, 6295−6303.
(33) Fuller, M. J.; Sinks, L. E.; Rybtehinski, B.; Giaimo, J. M.; Li, X. Y.; Wasielewski, M. R. *J. Phys. Chem. A* **2005**, *109*, 970−975.
(34) Kelley, R. F.; Rybtchinski, B.; Stone, M. T.; Moore, J. S.; Wasielewski, M. R. *J. Am. Chem. Soc.* **2007**, *129*, 4114−4115.
(35) Nelson, J. C.; Saven, J. G.; Moore, J. S.; Wolynes, P. G. *Science* **1997**, *277*, 1793−1796.
(36) Gin, M. S.; Yokozawa, T.; Prince, R. B.; Moore, J. S. *J. Am. Chem. Soc.* **1999**, *121*, 2643−2644.
(37) Prince, R. B.; Brunsveld, L.; Meijer, E. W.; Moore, J. S. *Angew. Chem., Int. Ed.* **2000**, *39*, 228−230.
(38) Balakrishnan, K.; Datar, A.; Zhang, W.; Yang, X. M.; Naddo, T.; Huang, J. L.; Zuo, J. M.; Yen, M.; Moore, J. S.; Zang, L. *J. Am. Chem. Soc.* **2006**, *128*, 6576−6577.
(39) Zhang, W.; Moore, J. S. *Angew. Chem., Int. Ed.* **2006**, *45*, 4416−4439.
(40) Ito, S.; Wehmeier, M.; Brand, J. D.; Kubel, C.; Epsch, R.; Rabe, J. P.; Mullen, K. *Chem.—Eur. J.* **2000**, *6*, 4327−4342.
(41) Wu, J. S.; Fechtenkotter, A.; Gauss, J.; Watson, M. D.; Kastler, M.; Fechtenkotter, C.; Wagner, M.; Müllen, K. *J. Am. Chem. Soc.* **2004**, *126*, 11311−11321.
(42) Simpson, C. D.; Wu, J. S.; Watson, M. D.; Müllen, K. *J. Mater. Chem.* **2004**, *14*, 494−504.
(43) Pisula, W.; Kastler, M.; Wasserfallen, D.; Pakula, T.; Müllen, K. *J. Am. Chem. Soc.* **2004**, *126*, 8074−8075.
(44) Mooney, W. F.; Brown, P. E.; Russel, J. C.; Costa, S. B.; Pedersen, L. G.; Whitten, D. G. *J. Am. Chem. Soc.* **1984**, *106*, 5659−5667.
(45) Whitten, D. G. *Acc. Chem. Res.* **1993**, *26*, 502−509.
(46) Song, X.; Geiger, C.; Leinhos, U.; Perlstein, J.; Whitten, D. G. *J. Am. Chem. Soc.* **1994**, *116*, 10340−10341.
(47) Whitten, D. G.; Chen, L.; Geiger, H. C.; Perlstein, J.; Song, X. *J. Phys. Chem. B* **1998**, *102*, 10098−10111.
(48) Nuckolls, C.; Katz, T. J.; Castellanos, L. *J. Am. Chem. Soc.* **1996**, *118*, 3767−3768.
(49) Shirakawa, M.; Fujita, N.; Tani, T.; Kaneko, K.; Shinkai, S. *Chem. Commun.* **2005**, 4149−4151.
(50) Kishimura, A.; Yamashita, T.; Aida, T. *J. Am. Chem. Soc.* **2005**, *127*, 179−183.
(51) Weng, W. G.; Beck, J. B.; Jamieson, A. M.; Rowan, S. J. *J. Am. Chem. Soc.* **2006**, *128*, 11663−11672.
(52) Camerel, F.; Ziessel, R.; Donnio, B.; Bourgogne, C.; Guillon, D.; Schmutz, M.; Iacovita, C.; Bucher, J. P. *Angew. Chem., Int. Ed.* **2007**, *46*, 2659−2662.
(53) Tam, A. Y. Y.; Wong, K. M. C.; Wang, G. X.; Yam, V. W. W. *Chem. Commun.* **2007**, 2028−2030.
(54) Baldo, M. A.; O'Brien, D. F.; You, Y.; Shoustikov, A.; Sibley, S.; Thompson, M. E.; Forrest, S. R. *Nature* **1998**, *395*, 151−154.
(55) Guo, F. Q.; Kim, Y. G.; Reynolds, J. R.; Schanze, K. S. *Chem. Commun.* **2006**, 1887−1889.
(56) Wong, W.-Y.; Wang, X.-Z.; He, Z.; Djurisic, A. B.; Yip, C.-T.; Cheung, K.-Y.; Wang, H.; Mak, C. S. K.; Chan, W.-K. *Nat. Mater.* **2007**, *6*, 521−527.
(57) Beljonne, D.; Wittmann, H. F.; Köhler, A.; Graham, S.; Younus, M.; Lewis, J.; Raithby, P. R.; Khan, M. S.; Friend, R. H.; Brédas, J.-L. *J. Chem. Phys.* **1996**, *105*, 3868−3877.
(58) Chawdhury, N.; Köhler, A.; Friend, R. H.; Wong, W.-Y.; Lewis, J.; Younus, M.; Raithby, P.; Corcoran, T. C.; Al-Mandhary, M. R. A.; Khan, M. S. *J. Chem. Phys.* **1999**, *110*, 4963−4970.
(59) Wilson, J. S.; Chawdhury, N.; Al-Mandhary, M. R. A.; Younus, M.; Khan, M. S.; Raithby, P.; Köhler, A.; Friend, R. H. *J. Am. Chem. Soc.* **2001**, *123*, 9412−9417.
(60) Rogers, J. E.; Cooper, T. M.; Fleitz, P. A.; Glass, D. J.; McLean, D. G. *J. Phys. Chem. A* **2002**, *106*, 10108−10115.
(61) Liu, Y.; Jiang, S.; Glusac, K.; Powell, D. H.; Anderson, D. F.; Schanze, K. S. *J. Am. Chem. Soc.* **2002**, *124*, 12412−12413.
(62) Glusac, K.; Kose, M. E.; Jiang, H.; Schanze, K. S. *J. Phys. Chem. B* **2007**, *111*, 929−940.
(63) Arnold, S.; Whitten, W. B.; Damask, A. C. *J. Chem. Phys.* **1970**, *53*, 2878−2884.
(64) Baessler, H.; Vaubel, G.; Kallmann, H. *J. Chem. Phys.* **1970**, *53*, 370−375.

and exciton transport in aggregates and films have been reported.[65] The PAOs that are the subject of this investigation provide an ideal platform for the study of triplet exciton transport and energy transfer. In particular, as described in this article, supramolecular aggregates consisting of **Pt2M** exhibit moderately intense phosphorescence from the platinum acetylide chromophore at ca. 500 nm. Interestingly, mixed aggregates consisting of **Pt2M** as the host with small amounts of **Pt2MT** exhibit phosphorescence emission predominantly from the latter chromophore, which emits at ca. 600 nm. Efficient sensitization of the phosphorescence from the low energy **Pt2MT** chromophores occurs via a mechanism involving triplet exciton diffusion among the aggregated **Pt2M** chromophores followed by energy transfer to the low energy **Pt2MT** acceptors. This study is the first to explore the properties of the triplet state and exchange energy transfer in supramolecular aggregates consisting of π-conjugated chromophores.

Experimental Section

Materials. Complete details concerning the synthesis and spectroscopic characterization of the platinum-acetylide oligomers are provided as Supporting Information. Solvents used for the spectroscopic measurements were spectral quality and were used without further purification.

Photophysical Measurements. Steady-state absorption spectra were recorded on a Varian Cary 100 dual-beam spectrophotometer. Samples were placed in a cell with a path length sufficiently short so as to maintain the absorption below 1.0 (1 or 0.1 mm path length). Corrected steady-state photoluminescence measurements were conducted on a SPEX F-112 fluorescence spectrometer. Samples were degassed by argon purging for 30 min and heated to a solution state regularly during this time for adequate degassing of gel-forming solutions. Samples were placed in a triangular-shaped cell that was positioned in the spectrometer so that the incident beam was at 45° from the face of the cell and emission detected at 45° (front-face geometry to minimize the effects of self-absorption). Time-resolved emission measurements were recorded on a home-built apparatus consisting of a nitrogen laser as a source ($\lambda = 337$ nm, 5 ns fwhm), with time-resolved detection provided by an intensified CCD detector (Princeton Instruments, PI-MAX iCCD) coupled to an Acton SpectraPro 150 spectrograph. Time-resolved spectra were analyzed by Global Kinetic Analysis using the Specfit/32 software package (Biologic SAS, www.bio-logic.info/rapid-kinetics/specfit.html). Circular dichroism (CD) spectroscopy was carried out on an Aviv-202 circular dichroism spectrometer with a cell path length of 0.3 mm.

Results

Chemical Structures, Gel Formation, and Gel Structure. The three platinum acetylide oligomers (PAOs) shown in Chart 1 are the focus of the work described herein. Each complex features an aromatic core moiety sandwiched between two *trans*-$Pt(P_2)(C_2)$ units, and the oligomer ends are capped with tri-(dodecyloxy)-substituted benzenes. Each of the PAOs induces gelation of hydrocarbon solvents such as *n*-dodecane, hexane, and cyclohexane.

Gelation was accomplished by mixing the PAO and solvent at ambient temperature, followed by warming the mixture to ca. 60 °C to produce a clear solution, followed by cooling to ambient temperature. Gelation typically occurred while the solution cooled (except for **Pt2MT**, see below). The critical gel concentration is approximately 1×10^{-3} M in dodecane and hexane for **Pt2M** and **Pt2MT** (~2 wt %), while it is 4×10^{-3} M for **Pt2MC**. For **Pt2M** and **Pt2MT** the gels formed quickly upon cooling a hot concentrated solution; however, gelation took approximately 3 days for a solution of **Pt2MC** in dodecane. Upon heating to ca. 50 °C, the gels melt to a clear nonviscous solution that could be reversibly brought back to the gel state upon cooling.

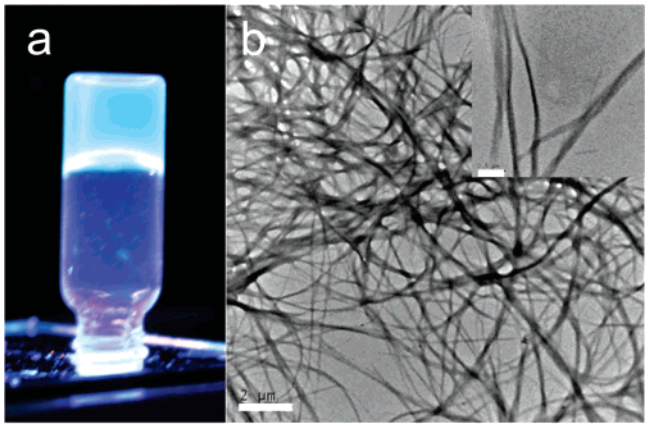

Figure 1. (a) Photograph taken of vial containing a gelled solution of **Pt2M** in dodecane ($c = 1$ mM). The photograph was taken with near-UV illumination, and a UV-blocking filter was placed in front of the camera lens. (b) Transmission electron microscope image of xerogel of **Pt2M** obtained by evaporation of dodecane solvent under vacuum, white scale bar is 2 μm in length. Inset shows the same sample under increased magnification; the white scale bar is 500 nm in length.

As shown in Figure 1, the gelated dodecane solution of **Pt2M** is rigid enough such that its flow is suppressed when the container is inverted.[66] The gelated material exhibits strong photoluminescence, and the spectroscopic properties of the emission are discussed below. In order to provide more insight into the morphology of the gelated **Pt2M** solution, TEM images were obtained on a zerogel sample that was prepared by drying of a film of a gel prepared in hexane. As can be seen in Figure 1b, the xerogel features a complex network of fibers consisting of the aggregated **Pt2M** molecules. The high-resolution image (inset, Figure 1b) shows that on average the widths of the individual fibers range from 50 to 200 nm. This suggests that the individual fibers are likely composed of many individual subfibers that consist of arrays of stacked **Pt2M** molecules. Close inspection of the enlarged TEM image suggests that the fibers may have a ribbon structure, which is consistent with the oligomers packing in a lamellar aggregate structure (*vide infra*).[67]

UV−visible Absorption Spectroscopy. Absorption spectra of the PAOs were measured in dodecane solution, and in each case the spectra were temperature- and concentration-dependent. For solutions with concentrations above 0.1 mM, the absorbance was maintained below a value of 1.0 by using short path length (1 mm or 0.1 mm) cells as necessary.

Figure 2a illustrates normalized absorption spectra of solutions of **Pt2M** in dodecane at three concentrations (1×10^{-4}, 5×10^{-4}, and 1×10^{-3} M). The solutions were subjected to a

(65) Haskins-Glusac, K.; Pinto, M. R.; Tan, C. Y.; Schanze, K. S. *J. Am. Chem. Soc.* **2004**, *126*, 14964−14971.

(66) The **Pt2M**/dodecane gel has the consistency of "jello". By comparison, the dodecane gels produced by **Pt2MT** and **Pt2MC** were somewhat less stiff, and with agitation they would "run". All of the gels exibited a slight opacity due to light scattering.

(67) Zubarev, E. R.; Pralle, M. U.; Sone, E. D.; Stupp, S. I. *J. Am. Chem. Soc.* **2001**, *123*, 4105−4106.

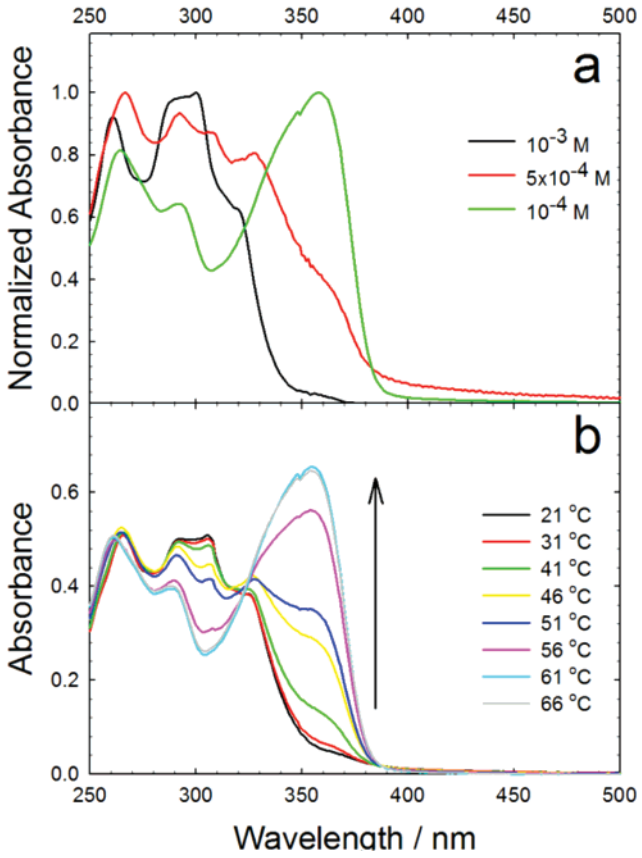

Figure 2. Absorption spectra of **Pt2M** in dodecane solution (or gel). (a) Room temperature. (b) $c = 10^{-3}$ M. Arrow indicates change in spectra with increasing temperature from 21 to 66 °C. The heating rate was approximately 1 °C min^{-1}, and spectra were acquired within 1 min after the temperature stabilized.

heating/cooling cycle before the spectra were obtained, but only the 1×10^{-3} M solution is in the gel state. The absorption spectrum of **Pt2M** in the dilute solution at 1×10^{-4} M (and below, data not shown) is dominated by a strong band with $\lambda_{max} = 358$ nm, with weaker transitions at higher energy (Figure 2a). The dominant absorption band is assigned to the long-axis polarized π,π^* transition of the molecularly dissolved (monomeric) chromophore.[61,62] Interestingly, when the concentration of **Pt2M** is increased above 10^{-4} M, the spectrum broadens and the primary oscillator strength shifts considerably to the blue. The spectrum of the solution with $c = 5 \times 10^{-4}$ M exhibits residual absorption in the region where the monomeric chromophore absorbs (shoulder at $\lambda \approx 365$ nm). By contrast, the spectrum of the gel of **Pt2M** with $c = 1 \times 10^{-3}$ M exhibits $\lambda_{max} \approx 304$ nm and there is very little residual absorption in the region where the monomer absorbs ($\lambda > 350$ nm). It is important that the spectrum observed for the **Pt2M**/dodecane gel is very similar to the spectra of H-aggregates of linear π-conjugated chromophores.[40,41,68]

Figure 2b illustrates the temperature dependence of the absorption spectrum of the **Pt2M** gel (solution) with $c = 10^{-3}$ M in dodecane. Upon heating the sample from 21 to 66 °C the absorption spectrum changes from that characteristic of the gel ($\lambda_{max} \approx 304$ nm) to that of the monomeric form of the complex ($\lambda_{max} = 358$ nm). (Over the same temperature range the sample undergoes a gel-sol transition.) It is also significant that there is an approximate isosbestic point maintained during the thermally induced transition, suggesting that the spectra are dominated by two principal forms of the oligomer, i.e., monomer at high temperature and H-aggregate at low temperature (gel). Note that the most significant changes in the absorption spectrum occur over the 40−60 °C temperature range, which brackets the temperature range of the sol−gel transition for **Pt2M** in dodecane. Similar concentration- and temperature-dependent behavior was observed for the absorption spectrum of **Pt2MT** in dodecane ($\lambda_{max}^{sol} = 378$ nm and $\lambda_{max}^{gel} = 338$ nm, see Supporting Information Figure S-1).

While **Pt2MC** also has the ability to gel dodecane, gelation occurs considerably more slowly than that for **Pt2M** and **Pt2MT**. The slow dynamics of aggregation/gelation are also apparent by the fact that the absorption spectral changes characteristic of the aggregate take several days to develop. As shown in the Supporting Information (Figure S-2), freshly prepared solutions with $c = 1 \times 10^{-4}$, 1×10^{-3}, and 4×10^{-3} M exhibit nearly identical absorption spectra, with $\lambda_{max} = 368$ nm (each solution was subjected to a heating−cooling cycle immediately prior to measuring the absorption spectrum). However, after standing for a period of several days the more concentrated solution gels, accompanied by a blue-shift of the UV absorption band to $\lambda_{max} = 345$ nm. The appearance of the gel/aggregate spectrum for **Pt2MC** is qualitatively similar to that of **Pt2M** and **Pt2MT**, suggesting that this complex also forms an H-aggregate. However, it is interesting that the spectral changes associated with H-aggregation of **Pt2MC** are less pronounced compared to the other two oligomers, suggesting that the exciton interactions are weaker. This is likely due to steric factors arising from the presence of the branched (and chiral) side groups present in **Pt2MC**.

Circular Dichroism Spectroscopy. Following the initial observation that **Pt2M** aggregates hydrocarbon solvents, presumably due to aggregation of the oligomers, we designed the structurally analogous oligomer **Pt2MC** with the objective of using CD to provide evidence for the existence of the supramolecular aggregates as well as to provide insight into structure of the aggregate.[3,4,12−14,20] **Pt2MC** has the same basic structure as **Pt2M**, with the exception that the central phenylene unit is substituted with optically active *S*-2-methylbutoxy side chains. We reasoned that by analogy to the chiral oligo(phenylene vinylene) aggregates[3,4,12−14,20] the supramolecular aggregates of **Pt2MC** would exhibit strong CD signals.

In initial experiments with **Pt2MC** it was observed that a freshly prepared, thermally cycled solution of the oligomer ($c = 4 \times 10^{-3}$ M) exhibits only a very weak CD signal (see Figure 3). However, as noted above, a freshly prepared solution of **Pt2MC** is not a gel, and the solution does not exhibit the absorption spectrum characteristic of the H-aggregate. However, if the thermally cycled solution is allowed to stand for ca. 3 days, the solution gels, and remarkably the gelled solution exhibits the strong CD spectrum shown in Figure 3. Several features are significant with this experiment. First, it clearly demonstrates that the CD signal is not a property of the monomeric chromophores—the signal is only observed when the sample is gelled and when the H-aggregate absorption spectrum is present. Second, the observation of the CD signal

(68) Schenning, A. P. H. J.; Kilbinger, A. F. M.; Biscarini, F.; Cavallini, M.; Cooper, H. J.; Derrick, P. J.; Feast, W. J.; Lazzaroni, R.; Leclere, P.; McDonell, L. A.; Meijer, E. W.; Meskers, S. C. J. *J. Am. Chem. Soc.* **2002**, *124*, 1269−1275.

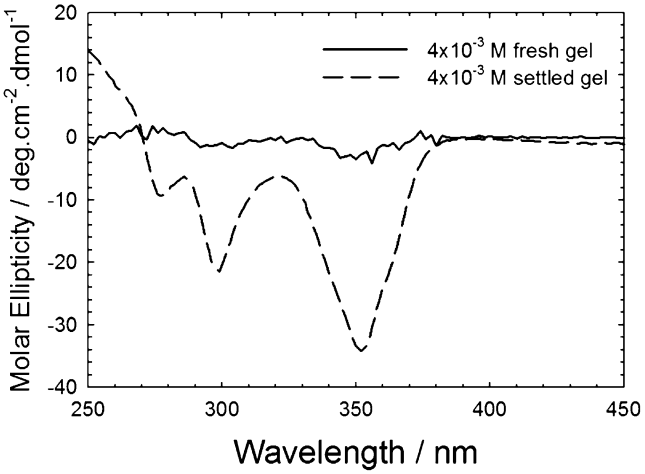

Figure 3. Circular dichroism spectra of **Pt2MC** in dodecane. Freshly prepared solution (—); gelled solution, 3 days after preparation (- - -).

for the **Pt2MC** aggregate signals that there is strong exciton coupling among the oligomer chromophores within a chiral, supramolecular environment provided by the aggregate.

The CD spectrum for the **Pt2MC** aggregate/gel primarily exhibits negative ellipticity throughout the near-UV spectral region where the aggregate absorbs. In particular, the CD features negative band maxima at 352, 295, and 272 nm, and each of these bands corresponds closely to the maxima of specific bands in the absorption spectrum of the **Pt2MC** H-aggregate (see Figure S-2). The observation of primarily negative ellipticity in the aggregate spectrum of **Pt2MC** contrasts with the CD spectra typically observed for the helical aggregates formed by chiral oligo(phenylene vinylene)s that have been previously studied.[3,4,12−14,20] In the latter case the CD spectra exhibit the bisignate CD signature typical for exciton coupling among a helical array of π-conjugated chromophores. The unusual CD spectrum observed for the **Pt2MC** aggregate/gel likely signals that the aggregate structure is not a helix. Although sufficient evidence does not exist to pinpoint the aggregate structure, it is possible that the negative ellipticity signals that the oligomers pack into a lamellar structure in the aggregate. The environment within the aggregate may be provided by a supramolecular twist in the lamellar structure or alternatively due to packing of the oligomers into a chiral subunit within the aggregate structure.[40,41]

Steady-State Photoluminescence Spectroscopy. Photoluminescence spectra of the platinum acetylide oligomers were measured in argon outgassed solutions (or gels). For the gels, the samples were warmed while degassing to prevent gel formation. Following degassing the solutions were cooled to produce degassed gels.

Figure 4 provides photoluminescence spectra of **Pt2M** obtained in dodecane gel (or solution) as a function of excitation wavelength, concentration, and temperature.[69] First, in all cases the **Pt2M** photoluminescence is dominated by a moderately efficient emission that is Stokes shifted significantly from the π,π^* absorption band. The emission has a lifetime in the microsecond time domain (*vide infra*), and on this basis it is

(69) Measurement of quantum yields and excitation spectra was precluded because the samples had a very high optical density and the emission experiments were carried out in a front-face geometry.

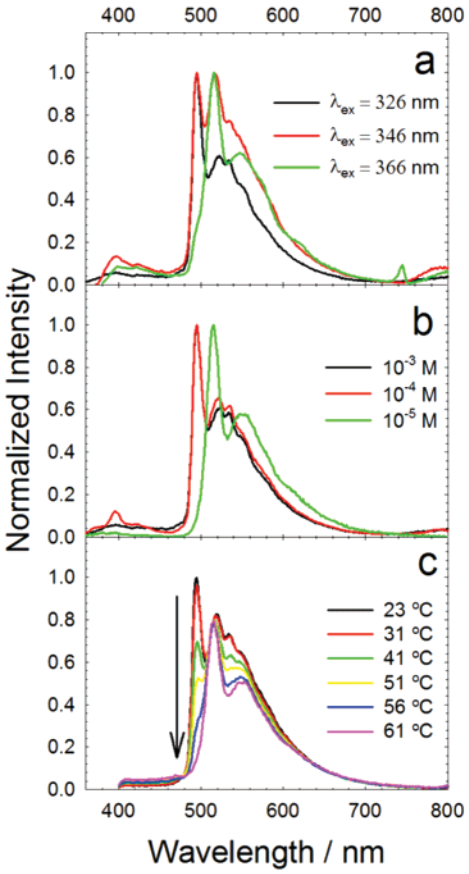

Figure 4. Photoluminescence spectra of **Pt2M** in deoxygenated dodecane. (a) $c = 1 \times 10^{-3}$ M. (b) $\lambda_{ex} = 326$ nm. (c) $\lambda_{ex} = 326$ nm and $c = 1 \times 10^{-3}$ M, from 23 to 61 °C. The arrow indicates the spectral change with increasing temperature. The heating rate was approximately 1 °C min^{-1}, and spectra were acquired within 1 min after the temperature stabilized.

assigned to phosphorescence from the $^3\pi,\pi^*$ state of the oligomer. The **Pt2M** phosphorescence is very similar in energy and band shape to the emission of structurally similar PAOs previously reported.[61,62] As shown in Figure 4a, the phosphorescence spectrum of **Pt2M** in the gel (1×10^{-3} M) depends on the excitation wavelength. In particular, with an excitation wavelength that corresponds to the absorption maximum for the gel ($\lambda = 326$ nm, cf. Figure 2a), the 0−0 band maximum of the phosphorescence is at 495 nm. However, with an excitation wavelength of 366 nm which corresponds to the absorption maximum for the molecularly dissolved state of the oligomer (cf. Figure 2a), the 0−0 band red-shifts to 516 nm. With an intermediate excitation wavelength $\lambda = 346$ nm, the phosphorescence consists of a broad manifold with two maxima at $\lambda = 495$ and 516 nm.

Several additional photoluminescence experiments provide insight concerning the origin of the excitation wavelength dependence seen for the **Pt2M** gel phosphorescence spectrum. First, as shown in Figure 4b, with excitation at 326 nm (corresponding to the absorption maximum of the aggregate) the 0−0 band of the phosphorescence appears at 516 nm for the most dilute solution ($c = 1 \times 10^{-5}$ M), whereas it blue-shifts to 495 nm for the two more concentrated solutions (1×10^{-4} and 1×10^{-3} M). Second, as shown in Figure 4c, warming a gelled solution of **Pt2M** (1×10^{-3} M) induces the 0−0 phosphorescence band to shift from 495 to 516 nm. The thermally induced red-shift in the phosphorescence is clearly

associated with the gel−sol transition. On the basis of these observations we attribute the "blue" phosphorescence (λ_{max} = 495 nm) to the **Pt2M** aggregates present in the gel and the "red" phosphorescence (λ_{max} = 516 nm) to the oligomer in the unaggregated (molecularly dissolved) state.

Several points are of interest with respect to the phosphorescence properties of **Pt2M**. First, the phosphorescence of both the aggregated and molecularly dissolved oligomers has a similar band shape, appearing as a distinct 0−0 transition with a shoulder on the low-energy side due to vibronic coupling. The important point is that the phosphorescence band shape is not strongly perturbed by close packing of the chromophores in the aggregates. This is in distinct contrast with the behavior typically seen when fluorescent chromophores are packed into an aggregate. In this case, the fluorescence spectra of the chromophores are strongly perturbed by exciton and eximer interactions, which signals that there is strong interaction between aggregated chromophores in the singlet excited state.[4,10] The fact that the aggregated state of **Pt2M** exhibits only a small shift in the phosphorescence energy is consistent with the notion that in the triplet excited state the oligomers interact only weakly with other chromophores in the aggregate. Importantly, there is no evidence for the existence of a triplet excimer in the **Pt2M** aggregates. This finding is consistent with previous studies which suggest that triplet excimer formation is not energetically favorable for aromatic chromophores.[70−72]

A second feature of interest is the fact that the changes in the phosphorescence spectrum that accompany the thermally induced gel−sol transition strongly suggest that there are two distinct "states" for the excited-state oligomer that exist in the gel and sol environments. In particular, the series of spectra shown in Figure 4c feature an isoemissive point, suggesting that as temperature increases (and the system undergoes the gel−sol conversion), the oligomers exist in two distinct states which give rise to either the 495 or 516 nm phosphorescence. On the basis of previous studies by our group on the temperature dependence of the phosphorescence emission of PAOs, we believe that the two states that give rise to the different phosphorescence emissions correspond to intramolecular conformations that differ with respect to the orientation of the phenylene and square planar $Pt(P_2)(C_2)$ units.[62] This issue will be considered more fully below in a later section.

Although the photoluminescence of **Pt2MT** was not studied extensively, qualitatively its emission responds to aggregation in a similar manner as that observed for **Pt2M**. First, in degassed solution **Pt2MT** ($c = 5 \times 10^{-5}$ M) exhibits phosphorescence that appears as a broad band with λ_{max} = 602 nm (see Figure S-3 in the Supporting Information). In the dodecane gel ($c = 1 \times 10^{-3}$ M) the phosphorescence band shape remains the same, but the band maximum shifts slightly to the blue (λ_{max} = 595 nm).

Time-Resolved Emission Spectroscopy. In order to provide further insight concerning the effects of aggregation on the triplet state of **Pt2M**, time-resolved photoluminescence experiments were carried out. In these studies the excitation source was a nitrogen laser (λ = 337 nm, 5 ns pulse width; note that this excitation wavelength corresponds closely to the absorption of the **Pt2M** aggregate), the emission was monitored using an intensified CCD camera/spectrograph system, and the emission decay kinetics were analyzed by global analysis[73] of the time-resolved spectra.

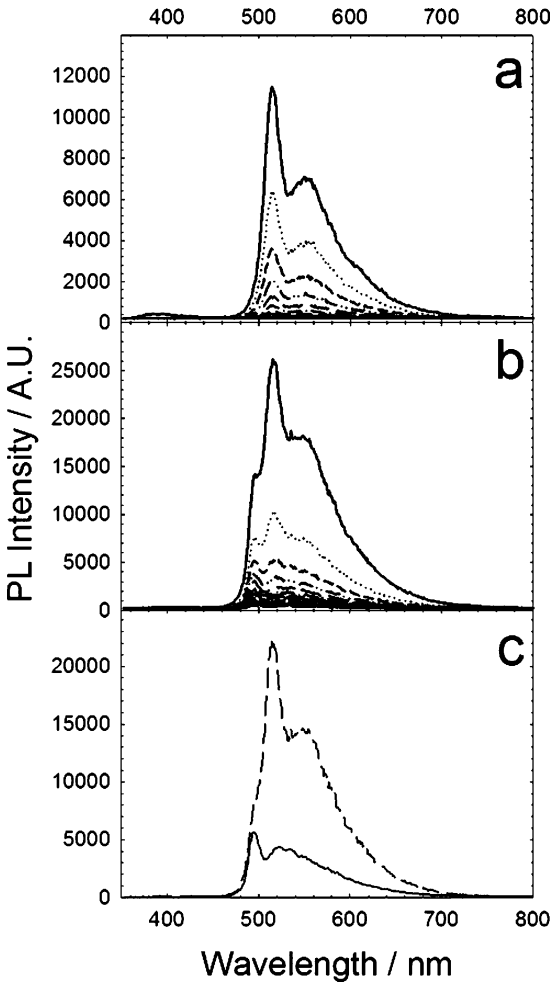

Figure 5. Time-resolved emission spectra of **Pt2M** in deoxygenated dodecane following pulsed excitation at λ_{ex} = 337 nm. (a) $c = 1 \times 10^{-5}$ M, 100 ns camera delay, 5.2 μs delay increment; (b) $c = 1 \times 10^{-3}$ M, 100 ns camera delay, 10.5 μs delay increment; (c) Principal components of emission decay of **Pt2M** at 1×10^{-3} M in dodecane for fast component τ = 9 μs (− −) and slow component τ = 59 μs (—).

Figure 5 illustrates the time-resolved emission data, and the decay parameters recovered from global analysis of the data are listed in Table 1. First, Figure 5a illustrates the time-resolved emission of **Pt2M** in a dilute (1×10^{-5} M) dodecane solution. The spectra were obtained with a delay increment of ca. 5 μs and the series of spectra shown in the figure were obtained over a time scale of ca. 50 μs. The emission spectrum does not change with time, and the λ_{max} (517 nm) and band shape are identical to those observed in the steady-state spectrum obtained for the dilute **Pt2M** solution where the emission occurs from the molecularly dissolved state of the oligomer. The emission decays as a single exponential with a lifetime of 10 μs, which is comparable to the lifetime of structurally similar PAOs.[61]

Figure 5b illustrates time-resolved spectra for **Pt2M** in a degassed dodecane gel ($c = 1 \times 10^{-3}$ M). These spectra were

(70) Lim, E. C. *Acc. Chem. Res.* **1987**, *20*, 8−17.
(71) Yanagidate, M.; Takayama, K.; Takeuchi, M.; Nishimura, J.; Shizuka, H. *J. Phys. Chem.* **1993**, *97*, 8881−8888.
(72) Yamaji, M.; Tsukada, H.; Nishimura, J.; Shizuka, H.; Tobita, S. *Chem. Phys. Lett.* **2002**, *357*, 137−142.
(73) Stultz, L. K.; Binstead, R. A.; Reynolds, M. S.; Meyer, T. J. *J. Am. Chem. Soc.* **1995**, *117*, 2520−2532.

Table 1. Phosphorescence Decay Lifetimes in Dodecane Solution or Gel[a]

complex	Pt2M			Pt2MT		Pt2M/Pt2MT
concn/M	1×10^{-5}	1×10^{-4}	1×10^{-3} [b]	1×10^{-5}	1×10^{-3} [b]	$1 \times 10^{-3}/5 \times 10^{-5}$ [b]
lifetime/μs	10	11	59 (22%)	5.2	23	5 (71%)
(amplitude%)			9 (78%)			41 (29%)

[a] Lifetimes in microseconds. Values in parentheses indicate relative amplitude of component. [b]Dodecane gel.

obtained with a delay increment of ca. 10 μs, and the series of spectra shown were obtained over a time scale of ca. 120 μs.

Interestingly, it can be seen that the shape of the spectrum evolves with time—the first few spectra (for $t < 30$ μs) are dominated by a band with $\lambda_{max} = 517$ nm, whereas at later delay times the spectra are dominated by the blue-shifted band with $\lambda_{max} = 495$ nm. Note that the longer-lived, blue-shifted emission band corresponds to the aggregated oligomer, while the red-shifted emission corresponds to the monomeric state. Global analysis of the time-resolved data shows that the emission decays with two exponential components ($\tau = 9$ and 59 μs), and the spectra of the two principal emission decay components recovered from the global analysis are shown in Figure 5c. The spectrum corresponding to the "fast" decay component (9 μs) has $\lambda_{max} \approx 517$ nm, and the spectrum corresponds closely to that of the monomeric **Pt2M**. Note that the lifetime of this component is very close to the lifetime of **Pt2M** in dilute solution (10 μs) supporting assignment of the "fast" decay component to molecularly dissolved **Pt2M**. The spectrum corresponding to the "slow" decay component (59 μs) is blue-shifted and has $\lambda_{max} \approx 495$ nm. This spectral-decay component clearly arises from the **Pt2M** aggregate. The considerably slower decay of the triplet state in the aggregate may arise because the microenvironment slows nonradiative decay (e.g., enhanced microviscosity, etc.). Alternatively, the lifetime may be increased because quenching by residual oxygen present in the solutions is slowed for the aggregated oligomers.

While the time-resolved emission spectrum of **Pt2MT** in a dodecane gel ($c = 1 \times 10^{-3}$ M, data not shown) does not display two emission bands as **Pt2M**, the lifetime is also much longer than is observed for the complex in dilute solution ($\tau = 23$ μs in gel versus 5.2 μs in 10^{-5} M solution). This observation is consistent with that for **Pt2M** in the gel, supporting the notion that the microenvironment present in the aggregates reduces the rate of nonradiative decay.

Energy Transfer in Mixed Gels Containing Pt2M and Pt2MT. A key objective of this study is to explore triplet−triplet energy transfer within the molecular aggregates consisting of the phosphorescent platinum-acetylide oligomers. The energy transfer experiments were designed by analogy to previous studies which indicate that singlet−singlet energy transfer is very efficient in molecular aggregates consisting of fluorescent, π-conjugated organic oligomers.[11,18,45,48,74] In the energy transfer experiments described below, **Pt2M** serves as the "host" and the energy donor, while **Pt2MT** serves as the energy acceptor (i.e., the energy "trap"). Energy transfer from **Pt2M** to **Pt2MT** is moderately exothermic, since the triplet energy of **Pt2M** is ca. 0.45 eV above that of **Pt2MT**.

Emission spectroscopy was used to monitor the energy transfer process in the mixed gel solutions. First, Figure 6 summarizes the results of a series of steady-state emission experiments carried out on dodecane gels containing **Pt2M** at a fixed concentration (1×10^{-3} M) with varying amounts of **Pt2MT** added (0−5 mol %, concentration range $(0-5) \times 10^{-5}$ M).[75] The excitation wavelength (300 nm) was carefully selected such that in each case the light is absorbed almost exclusively (≥95%) by the **Pt2M** donor chromophore.[76] As can be seen in the spectra, as the amount of **Pt2MT** added to the gel increases, the red phosphorescence ($\lambda_{max} \approx 580$ nm) from **Pt2MT** rapidly increases in intensity, to the point where it dominates the spectra for ≥4 mol % added. A control experiment using the same concentration of **Pt2MT** alone in dodecane ($c = 5 \times 10^{-5}$ M) with 300 nm excitation gave virtually no phosphorescence signal. A second control experiment was carried out in a chloroform solution containing **Pt2M** and **Pt2MT** ($c = 1 \times 10^{-3}$ and 5×10^{-5} M, respectively). In chloroform **Pt2M** is molecularly dissolved even at high concentration, and regardless of the excitation wavelength only emission from **Pt2M** is observed.

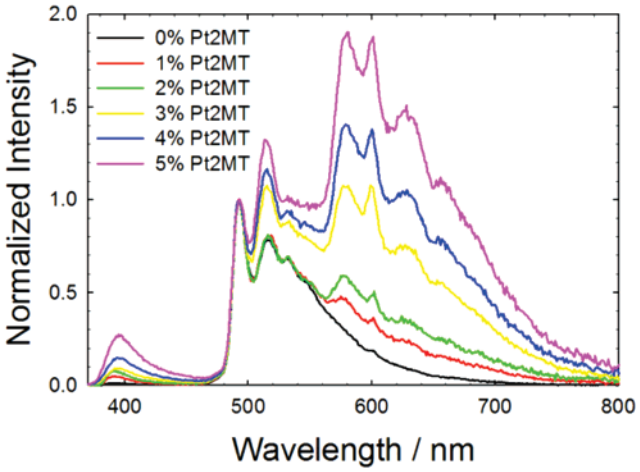

Figure 6. Photoluminescence spectra of **Pt2M**−**Pt2MT** mixed-oligomer gel in deoxygenated dodecane. [**Pt2M**] = 1×10^{-3} M and different mol % of **Pt2MT**, $\lambda_{ex} = 300$ nm. Spectra are normalized at 495 nm.

Taken together, the results on the mixed dodecane gels (and chloroform solution) clearly indicate that the **Pt2MT** phosphorescence emission arises via a mechanism involving triplet energy transfer from **Pt2M** which acts as a "sensitizer". In addition, the process only occurs when the PAOs are aggregated, suggesting that exciton diffusion among the **Pt2M** units is involved. Note that the emission spectra in Figure 6 are normalized at 495 nm (the wavelength corresponding to the **Pt2M** aggregate emission). With this normalization in mind, comparison of the spectra with increasing **Pt2MT** concentration

(74) Daniel, C.; Herz, L. M.; Beljonne, D.; Hoeben, F. J. M.; Jonkheijm, P.; Schenning, A. P. H. J.; Meijer, E. W.; Phillips, R. T.; Silva, C. *Synth. Met.* **2004**, *147*, 29−35.

(75) TEM images of a xerogel produced from the **Pt2M**/**Pt2MT** (5 mol%) mixture are provided in the Supporting Information.

(76) At 300 nm, the molar absorptivity of **Pt2M** and **Pt2MT** is 50 000 and 35 000 M^{-1} cm^{-1}, respectively. Thus, at 300 nm for an equimolar solution of **Pt2M** and **Pt2MT** the ratio of light absorption by the two chromophores is ≈1.4:1. For the mixed gel containing the highest mole fraction of **Pt2MT** used (5 mol%), the **Pt2M**/**Pt2MT** light absorption ratio is 29:1 at 300 nm.

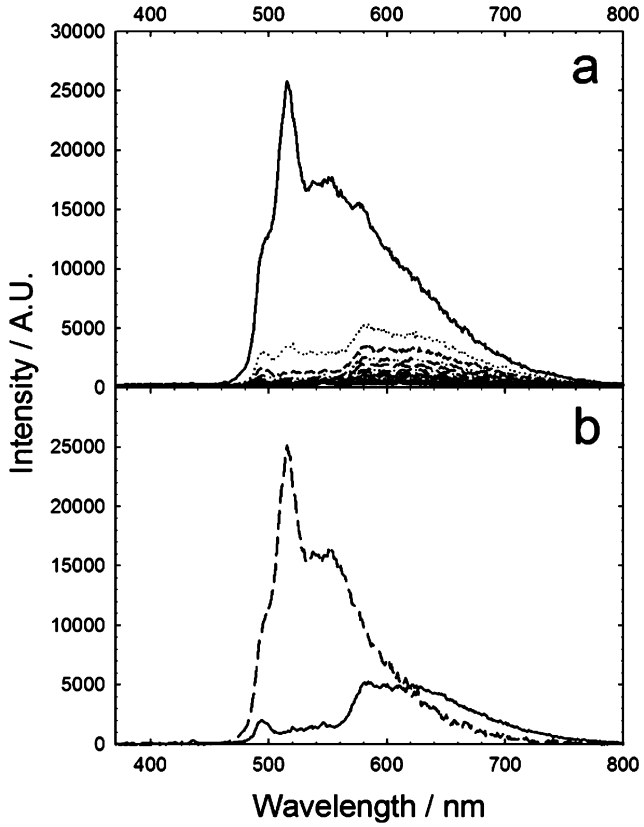

Figure 7. Time-resolved emission spectra of **Pt2M** with 5 mol % **Pt2MT** in deoxygenated dodecane gel following pulsed excitation at $\lambda_{ex} = 337$ nm. (a) Initial spectrum obtained at 1 μs delay and succeeding spectra obtained with 10.5 μs delay increments. (b) Principal components of emission decay of **Pt2M** at 1×10^{-3} M with 5 mol % **Pt2MT** in dodecane for fast component $\tau = 5$ μs (− −) and slow component $\tau = 41$ μs (—).

reveals that the **Pt2M** monomer emission intensity (516 nm) increases relative to that of the **Pt2M** aggregate (495 nm). This suggests that the **Pt2MT** acceptor quenches the phosphorescence from the **Pt2M** aggregate more efficiently than the **Pt2M** aggregate which is in free solution. As discussed below, this notion is at least qualitatively consistent with a model in which triplet exciton transport and energy transfer occur within aggregates consisting of **Pt2M** as the host and **Pt2MT** as the energy trap.

The phosphorescence dynamics of the **Pt2M**/**Pt2MT** mixed oligomer system were explored using time-resolved emission (with 337 nm excitation) in order to gain insight concerning the dynamics of energy transfer. Figure 7a shows time-resolved emission spectra of a dodecane gel containing of **Pt2M** ($c = 1 \times 10^{-3}$ M) and 5 mol % **Pt2MT** ($c = 5 \times 10^{-5}$ M). The series was obtained with a delay increment of ca. 10 μs, and the spectra shown were obtained over a time scale of ca. 100 μs. Interestingly, the first spectrum (obtained with a 1 μs delay from laser pulse) is dominated by the **Pt2M** phosphorescence; however, succeeding spectra (delay ≥ 10 μs) are dominated by the phosphorescence of **Pt2MT**. The results provide very clear qualitative support for the notion that the triplet state of **Pt2M** is quenched efficiently by energy transfer to **Pt2MT**.

Global analysis of the time-resolved emission data provides insight into the energy transfer dynamics in the mixed aggregates. The analysis affords two principal decay components: "fast" with $\tau \approx 5$ μs and "slow" with $\tau \approx 41$ μs. The principal component spectra corresponding to the two decay components are shown in Figure 7b. The spectrum of the fast lifetime component is dominated by the phosphorescence from the **Pt2M** (donor) chromophores, whereas the spectrum corresponding to the slow component is dominated by phosphorescence from the **Pt2MT** (acceptor), with a small contribution from the aggregate band ($\lambda = 495$ nm) of **Pt2M**. Several points are significant with respect to the time-resolved emission data. First, it is evident that the **Pt2M** phosphorescence decays more rapidly in the presence of **Pt2MT**; virtually all of the **Pt2M** emission decays with $\tau \approx 5$ μs. This is much faster than the natural decay of the **Pt2M** aggregate state ($\tau \approx 59$ μs), suggesting that the **Pt2M** to **Pt2MT** energy transfer occurs rapidly and efficiently in the mixed aggregate system. The second important point is that the lifetime of the **Pt2MT** phosphorescence (the slow component) in the mixed gel is *longer* than that observed in the pure **Pt2MT** aggregates (41 μs versus 23 μs). The observation further supports the notion that the phosphorescence from **Pt2MT** is being sensitized by the **Pt2M** donor chromophores in the aggregates.

Discussion

Aggregates of π-Conjugated Oligomers. Before considering the aggregation and photophysical properties of the platinum acetylide oligomers (PAOs), it is important to briefly summarize relevant prior work on aggregates and organogels consisting of supramolecular assemblies of organic π-conjugated oligomers. This review is significant because it provides insight relevant to the results obtained on the PAOs that are the focus of the present study.

As noted above, Meijer investigated the solution and optical properties of a series of oligo(phenylene vinylene)s (OPVs) end-capped with trialkoxybenzene units. The OPVs self-assemble into supramolecular assemblies that are proposed to consist of helical arrays of stacked π-conjugated chromophores.[4] The arrays are stabilized by solvophobic and $\pi-\pi$ interactions between the stacked aromatic chromophores.[3] Aggregation of the OPVs is accompanied by a slight red-shift in their π,π^* absorption and a more pronounced red-shift and broadening of the fluorescence. The change in fluorescence is attributed to emission from an "excimer like" state arising from π-stacking of the chromophores in the aggregates. The OPVs are substituted with chiral aliphatic side chains, and the supramolecular aggregates exhibit a strong, bisignate CD spectrum arising from exciton coupling of the chromophores within the chiral aggregate. The bisignate CD is typical of π-conjugated chromophores that are in a helical environment. More recently, Ajayghosh studied a series of hydroxymethyl-substituted OPVs that produce stable organogels in hydrocarbon solvents.[10,20] Gelation occurs due to the formation of nanofibers consisting of supramolecular assemblies of the OPVs stabilized by hydrogen bonding and $\pi-\pi$ stacking interactions between the π-conjugated chromophores. The hydroxymethyl-substituted OPVs undergo very similar changes in absorption and fluorescence concomitant with aggregation and gelation as described by Meijer for his supramolecular OPV aggregates, and they also exhibit strong bisignate CD spectra signaling that the aggregate provides a chiral environment.

Another series of investigations relevant to the results reported here is work by Whitten and co-workers on aggregates consisting of stilbene-functionalized phospholipids.[39−41] The absorption

and fluorescence properties of the stilbene-phospholipids were studied in Langmuir monolayer films and in bilayer vesicles. In these lipid assemblies the stilbene chromophores exist in a chiral H-aggregate structure characterized by a strongly *blue-shifted* absorption and a slightly red-shifted fluorescence. Crystal structures and molecular dynamics simulations suggest that the stilbene aggregates consist of a glide layer structure that features chiral "pinwheel" or "herringbone" units consisting of four chromophore assemblies that interact predominantly via non-covalent edge-to-face interactions of the stilbenes.[40]

Structure of Platinum Acetylide Aggregates. The optical and materials data show that in hydrocarbon solvents at concentrations above 1×10^{-4} M **Pt2M**, **Pt2MT**, and **Pt2MC** form supramolecular aggregates, and when the concentration is above 1×10^{-3} M aggregation leads to gelation of the solutions. Since the PAO structures are analogous to the aggregating OPVs previously studied (i.e., they consist of rigid, π-conjugated cores capped on each end by trialkoxybenzene units),[4] it is compelling to suggest that the structure of the PAO aggregates is similar to those produced by the OPVs. Specifically, the PAOs take on an overall planar conformation, packing into a supramolecular "card stack" that has a helical twist giving rise to the chiral environment that is signaled by the observed strong CD spectrum.

However, there are important differences in the spectroscopic properties when comparing the OPV and the PAO aggregates, and these differences suggest that the manner in which the oligomers pack in the aggregates is different, leading to a different supramolecular structure. First, the OPV aggregates exhibit a red-shifted absorption and broad, red-shifted "excimer-like" fluorescence.[4,10] Thus, the spectroscopy of the OPV aggregates is apparently dominated by the $\pi-\pi$ interchromophore interactions that arise when the relatively planar OPV chromophores π-stack in the card pack aggregate structure. By contrast, **Pt2M**, **Pt2MT**, and to a lesser extent **Pt2MC** exhibit a significantly *blue-shifted* absorption with little perturbation of the phosphorescence emission. These features suggest that the spectroscopy of the aggregated PAOs is dominated by relatively weaker excitonic interactions between the chromophores. An important point is that the absorption spectrum of the **Pt2M** aggregate, which has been attributed to an H-aggregate, is remarkably similar to that of the stilbene H-aggregates reported by Whitten.[40] In the stilbene aggregates the absorption and emission spectra are also dominated by exciton coupling among the chromophores, as there is little evidence for the existence of "excimer like" fluorescence.[40] As noted above, in the stilbene aggregates the interchromophore interactions are dominated by edge-to-face interactions between the aryl rings, as opposed to $\pi-\pi$ stacking. The similarity of the spectroscopy of the stilbene and PAO aggregates suggests that in the latter the chromophores pack in a way such that $\pi-\pi$ interactions are not significant. This is consistent with the fact that the PAOs are less likely to adopt an all-planar structure (see below) and with the presence of the comparatively bulky PMe_3 ligands on the platinum centers.

A second important feature concerns the origin of the ca. 20 nm blue-shift in the phosphorescence that is seen for the **Pt2M** aggregate relative to the molecularly dissolved state (λ_{max} shifts from 516 to 495 nm). As noted above, the spectral shift is believed to arise due to a difference in the conformation of the triplet excited state in the aggregate relative to that in the molecularly dissolved state. This conclusion is based on previous studies where we examined the temperature dependence of the phosphorescence for a series of PAOs that are structurally similar to **Pt2M**.[62] Of particular significance to the present work is the temperature dependence of the phosphorescence for the complex *trans*,*trans*-[Ph—C≡C—Pt$(PBu_3)_2$—C≡C—(1,4-Ph)—C≡C—Pt$(PBu_3)_2$—C≡C—Ph] (**Pt2**, where Ph is phenyl and 1,4-Ph is 1,4-phenylene).[62] Note that **Pt2** has the same chromophore as **Pt2M** but it lacks the trialkoxy groups on the terminal phenyl groups. The phosphorescence of **Pt2** was investigated in dilute 2-methyltetrahydrofuran (MTHF) solution over the temperature range from 300 to 80 K. Above the glass point of MTHF (ca. 120 K) the emission of **Pt2** is very similar to that of **Pt2M** in dilute solution with a single 0−0 band at $\lambda_{max} = 519$ nm. However, at temperatures below 120 K where the MTHF is a rigid glass, the emission of **Pt2** exhibits an additional 0−0 band that is blue-shifted to $\lambda_{max} = 497$ nm. Excitation wavelength studies demonstrate that the two emission 0−0 bands arise from two distinct triplet states of **Pt2** that do not interconvert in the glass. On the basis of density functional theory (DFT) calculations these two emitting states were identified as differing in the conformation of the central phenylene unit. The low-energy emission ($\lambda_{max} = 519$ nm) arises from the conformation of the triplet state in which the central phenylene ring is oriented coplanar relative to the planes defined by the square planar PtP_2C_2 units. The higher energy emission ($\lambda_{max} = 497$ nm) arises from the conformer in which the central phenylene ring is perpendicular to the planes defined by the square planar PtP_2C_2 units. These two conformers are illustrated in Scheme 1 and are labeled **p** and **t**, respectively. DFT calculations indicate that for **Pt2** the **p** conformer is the most stable conformer in the triplet state, whereas **t** is the most stable in the ground state.

Scheme 1

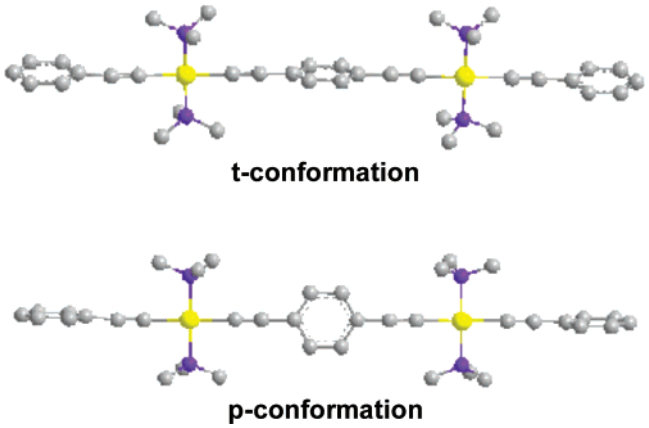

The implications of the observations on **Pt2** in the MTHF solvent glass are obvious—the high-energy phosphorescence observed from **Pt2M** in the aggregates ($\lambda_{max} = 495$ nm) must arise from the **t** conformer, whereas the low-energy emission observed from the molecularly dissolved complex ($\lambda_{max} = 516$ nm) arises from the **p** conformer. When **Pt2M** is molecularly dissolved, following initial excitation and intersystem crossing to the triplet state, the oligomer is able to rapidly relax into the energetically preferred **p** conformer prior to emission. By contrast, in the aggregate **Pt2M** is sterically constrained so that conformational relaxation cannot occur in the triplet excited

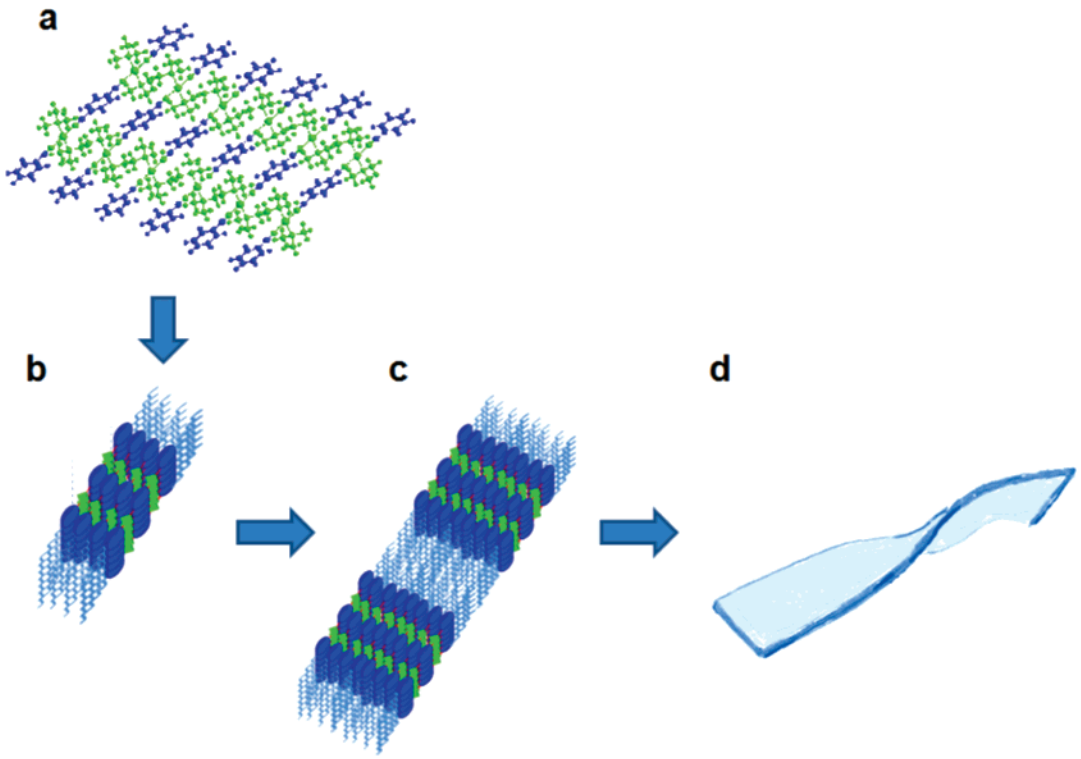

Figure 8. Schematic illustrating possible arrangement of **Pt2M** units within supramolecular aggregate: (a) Sheetlike packing of individual monomers in **t**-conformation, (b) stacking of sheets, (c) lamellar packing of stacked sheets, and (d) ribbon with supramolecular twist.

state. Consequently for the **Pt2M** aggregates the emission occurs from the unrelaxed **t** conformation. It follows from this that in the aggregate the **Pt2M** oligomers are present in the **t** conformation.

Although it is only possible to speculate as to how the PAOs pack in the aggregates, on the basis of the spectroscopic data and its relationship to the other π-conjugated oligomer aggregates, we suggest the model shown in Figure 8 as one possible motif. In this model the individual PAOs are in the **t** conformation, packing into a slipped stack arrangement (Figure 8a). The individual sheets may stack and assemble into a lamellar sheet structure (Figure 8b and c). Finally, on a longer length scale the lamellar sheet may produce a ribbon structure which is twisted (in a helical sense), giving rise to the optical activity that is observed for the **Pt2MC** aggregates. This packing model is consistent with the observation that H-aggregate exciton coupling is the dominant interchromophore interaction.[77,78] It also would explain the observation that in the triplet excited state the conformation of the oligomers is constrained from undergoing the **t** → **p** relaxation, as the slipped stack structure (Figure 8a) is sterically constrained such that rotation of the individual phenylene rings is precluded.

Triplet Energy Transfer in the Pt2M/Pt2MT Mixed Gels. The study of the mixed aggregates provides clear evidence for the occurrence of triplet energy transfer from **Pt2M** (donor/host) to **Pt2MT** (acceptor/trap). First, energy transfer is only observed when the mixed oligomers are in the aggregates. This conclusion is based on the fact that while energy transfer occurs for the mixed aggregates in dodecane solution (Figure 6), it

Scheme 2

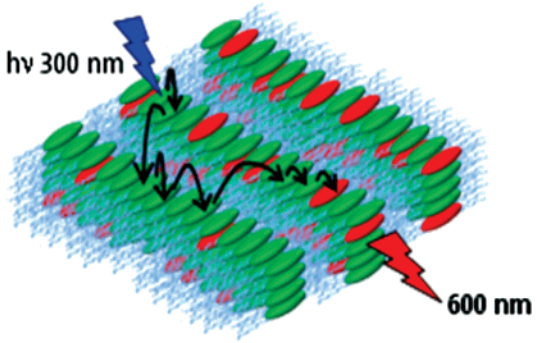

does not occur in a chloroform solution that contains the same **Pt2M** and **Pt2MT** concentrations (the oligomers do not aggregate in $CHCl_3$). Second, the photophysical results indicate that triplet energy transfer is relatively efficient, even when the acceptor is present at a low concentration (i.e., 1 − 2 mol %) in the aggregates.

While the structure of the mixed aggregates at the molecular level is not known, it is likely that even when the **Pt2MT** trap is present at the 5 mol % level (i.e., the ratio of **Pt2M**/**Pt2MT** is 20:1) the median distance between the traps is greater than 25 Å. In view of this fact, given that the rate of triplet (exchange) energy transfer falls exponentially with distance,[79] we conclude that energy transfer within the mixed aggregates occurs via a mechanism involving diffusion of the exciton within the **Pt2M** host aggregate until it encounters a **Pt2MT** acceptor site where it becomes trapped (Scheme 2). Exciton diffusion within the aggregate must occur via a random walk wherein the triplet excitation hops between adjacent **Pt2M** monomers via a Dexter

(77) McRae, E. G.; Kasha, M. In *Physical Processes in Radiation Biology*; Augenstein, L., Mason, R., Rosenberg, B., Eds.; Academic Press: New York, 1964; pp 23−42.
(78) Kasha, M.; Rawls, H. R.; Ashraf El-Bayoumi, M. *Pure Appl. Chem.* **1965**, *11*, 371.
(79) Dexter, D. L. *J. Chem. Phys.* **1953**, *21*, 836−850.

exchange triplet energy transfer mechanism.[79] While the dynamics of the triplet hopping and trapping steps are not known with certainty, the time-resolved emission studies indicate that the overall exciton diffusion/trapping process occurs on the 1−10 μs time scale. This suggests that the time scale for triplet exciton hopping between the individual **Pt2M** oligomers in the aggregate occurs on the nanosecond time scale (e.g., site-to-site hopping rate on the order of 10^7-10^8 s^{-1}). This hopping rate is significantly less than the rate of singlet exciton migration in aggregates which occurs on a time scale of $10^{10}-10^{11}$ s^{-1}.[48] The much slower rate of triplet exciton hopping is consistent with a mechanism involving Dexter exchange energy transfer between weakly coupled monomers.[79]

Summary and Conclusions

A series of platinum acetylide oligomers designed to self-assemble in hydrocarbon solvents was synthesized with the primary objective of studying the consequences of aggregation on the triplet excited state. The PAOs feature a rigid-rod linear platinum acetylide chromophore end-capped with tridodecyloxyphenyl units. Each of the oligomers aggregates in hydrocarbon solvents, and at sufficiently high concentration (ca. 2 wt. %) aggregation leads to gelation.

Comparison of the photophysics of the PAOs in solution and in the aggregates provides insight into the molecular and supramolecular structure of the aggregates. The absorption spectra of the aggregated oligomers are blue-shifted significantly compared to the absorption when they are molecularly dissolved. The blue shift is attributed to exciton coupling within a supramolecular structure in which the chromophores are packed into a H-aggregate array. The phosphorescence of the aggregated PAOs is blue-shifted only slightly compared to the molecularly dissolved state, indicating a triplet excimer is not produced in the aggregates. The phosphorescence blue shift is attributed to emission from a high energy (molecular) conformation that is unable to undergo geometric relaxation in the constrained environment presented by the aggregate structure.

The spectroscopic studies indicate that Pt−Pt interactions are not important in the aggregate structures. This finding contrasts with recent work on supramolecular aggregates consisting of square planar platinum terpyridine chromophores, where Pt−Pt interactions are believed to play a significant role in the aggregation (and gelation) behavior of the complexes.[52,53] In the platinum terypyridine systems, aggregation is accompanied by development of new low-energy absorption and emission bands. These bands are attributed to a charge-transfer excited state based on promotion of an electron from a metal−metal bonding orbital into the terpyridine ligand (metal−metal to ligand charge transfer, MMLCT). The lack of significant Pt−Pt interactions in the **Pt2M** aggregates is consistent with the fact that the platinum centers are sterically congested by the PMe_3 ligands.

Efficient triplet−triplet energy transfer is observed in mixed aggregates consisting of **Pt2M** as the donor/host and **Pt2MT** as the acceptor/trap. Energy transfer is only observed when the mixed oligomer system is in the aggregate/gel state, indicating that exciton diffusion within the **Pt2M** host is important in transporting the exciton to a **Pt2MT** trap. This work provides the first example of the observation of triplet exciton diffusion and trapping in a molecular aggregate system. Ongoing experiments in our laboratory seek to provide quantitative insight into the efficiency and dynamics of triplet exciton diffusion and trapping in phosphorescent aggregates consisting of platinum acetylide chromophores.

Acknowledgment. We thank the National Science Foundation for support of this research (Grant No. CHE-0515066). We acknowledge Dr. Kye-Young Kim for assistance with the graphics.

Supporting Information Available: Full experimental section, including description of synthesis of **Pt2M**, **Pt2MT**, and **Pt2MC** with complete spectral characterization data (^1H, ^{13}C, and ^{31}P NMR spectra), temperature dependent absorption spectra of **Pt2MT**, concentration dependent absorption spectra of **Pt2MC**, concentration dependent phosphorescence spectra for **Pt2MT**, and TEM images of xerogels of **Pt2M/Pt2MT** mixture (2 Schemes, 13 Figures). This material is available free of charge via the Internet at http://pubs.acs.org.

JA0765316